

Synthesis and characterization of Fe(III)-doped ceramic membranes of titanium dioxide and its application in photoelectrocatalysis of a textile dye

Emanuel C. Rodrigues ^{a1}, Layciane. A. Soares ^a, Marco A. Modenes Jr ^a, Jeosadaque J. Sene ^a, Gilbert Bannach ^b, Claudio T. Carvalho ^c and Massao Ionashiro ^c.

^{a*} Centro Universitário da Fundação Educacional de Barretos, UNIFEB, CEP 14780-226, Barretos, SP, Brazil; emanuelbarretos@bol.com.br.

^b Instituto de Química, UNESP, CEP 17033-360, Bauru, SP, Brazil.

^c Instituto de Química, UNESP, C.P. 355, CEP 14801-970, Araraquara, SP, Brazil.

Abstract

Pure and Fe(III)-doped TiO₂ suspensions were prepared by the sol gel method with the use of titanium isopropoxide (Ti(OPri)₄) as precursor material. The properties of doped materials were compared to TiO₂ properties based on the characterization by thermal analysis (TG-DTA and DSC), X-ray powder diffractometry and spectroscopy measurements (FTIR). Both undoped and doped TiO₂ suspensions were used to coat metallic substrate as a mean to make thin-film electrodes. Thermal treatment of the precursors at 400°C for 2 h in air resulted in the formation of nanocrystalline anatase TiO₂. The thin-film electrodes were tested with respect to their photocatalytic performance for degradation of a textile dye in aqueous solution. The plain TiO₂ remains as the best catalyst at the conditions used in this report.

Keywords: TiO₂; Fe(III) doping; characterization; thin film electrode; textile dye.

Introduction

Titanium dioxide (TiO_2) is a polymorphous crystalline solid which exists in a tetragonal phase as anatase and rutile, as well as, in a rhombic phase called brookite. The most common forms, anatase and rutile, are easily prepared as ceramic membranes by several methods of synthesis [1].

Accordingly, the sol-gel method allow to the preparation of ceramic materials such as powders, fibers and membranes at relatively low temperature when compared to conventional methods. Also, metal-doped materials can be prepared in such a way that the stoichiometry, particle size and porosity are controllable. Such materials have been characterized by a number of different techniques as thermal analysis (thermogravimetry (TG), differential thermal analysis (DTA), and differential scanning calorimetry (DSC)), X-ray diffraction, scanning electronic microscopy, and spectroscopy techniques [2-14].

TiO_2 ceramic membranes have been widely used as a photocatalyst to degrade pollutants in aqueous phase, as well as, in the gaseous one. For that purpose, the semiconductor must be activated by light of energy greater than the band gap energy of the material which can be accomplished by the use of artificial lighth or better yet by solar energy. The activation gives rise to the formation of electrons in the conduction band and positive holes in the valence band, these being responsible for the oxidation of organic matter [15].

Some reviews on the use of titanium dioxide (TiO_2) as a photocatalyst are available in the literature, which present the current progress in the field as well as a discussion of the fundamental aspects [16-18].

The photocatalytic efficiency of TiO_2 is influenced by its structure, defects and impurities, as well as, by its superficial morphology and interface. These aspects depend on the method of preparation and the firing temperature, which in turn define the composition of the crystal phase in the final material. Generally, the rutile phase is claimed to be less photoactive than anatase. The addition of small amounts of a metal doping to the bulk phase of TiO_2 is meant to increase its photocatalytic efficiency and promote a red shift in the band gap energy. Results of several doping-metals such as Al, Cd, Ce, Co, Cr, Fe, Li, Mn, Ni, Pt, Zn and V have been reported [19-21].

Iron (III) ions have been demonstrated to improve the catalytic activity of TiO₂ toward the oxidation of organic pollutants. These results are encouraging since the properties of TiO₂ photocatalysts are suitable for the construction of photochemical energy conversion systems and the treatments of pollutants and wastewater [22-27]. Several studies have claimed that TiO₂ as anatase coexists with metallic iron at acidic pH or in situations where the doping level of iron is less than 1% (m/m) which enhance the photocatalytic properties of TiO₂. As the doping level goes higher or at higher pH, the phase α -Fe₂O₃ has much more probability to form which cause the transformation of TiO₂ from anatase to rutile [28-31].

In this paper studies on the preparation of Fe(III)-doped TiO₂ are described. Materials with the percentage of metal doping of 1%, 5% and 10% were synthesized and their properties compared to those of plain TiO₂ based on the characterization by thermal analysis and spectroscopy measurements. In addition, thin-film electrodes made out these materials were used to photoelectrocatalytically degrade a textile dye in aqueous solution.

2. Experimental

2.1 Materials

Titanium sol was prepared by adding titanium isopropoxide, Ti(OPri)₄ (Aldrich, Milwaukee, WI), to an aqueous solution of nitric acid at a volumetric mixing ratio of 2.1 mL concentrated HNO₃/238 mL H₂O/20 mL Ti(OPri)₄. The sol was stirred continuously until peptization was complete, after which the sol (pH 1.0) was dialyzed (Spectra/Por1 3 membrane, 3500 MW cutoff, Spectrum, Laguna Hills, CA) to a final pH 3.5. The iron-doped sols were prepared by a similar procedure with the addition at the initial step of the required amount of iron (III) nitrate to obtain 1, 5 and 10% atom ratio of iron to titanium.

2.2 Methods

Simultaneous TG-DTA and DSC curves were recorded in models SDT 2960 and Q 10, both from TA instruments and TG Mettler TA-4000 thermal analysis system (TiO₂ undoped). The purge gas was an air flow of 100 mL min⁻¹ for TG-DTA and 50 mL min⁻¹ for DSC. A heating rate of 20°C min⁻¹ was adopted with samples weighing about 7 mg for TG-DTA and 5

mg for DSC. Alumina and aluminum crucibles, the latter with perforated covers, were used for TG-DTA and DSC, respectively.

Infrared spectra were recorded on a Nicolet mod. Impact 400 FT-IR instrument, within the 4000–400 cm^{-1} range. The solid state samples were pressed into KBr pellets.

X-ray powder patterns were obtained by using a Siemens D-5000 X-Ray Diffractometer, employing $\text{CuK}\alpha$ radiation ($\lambda=1.541 \text{ \AA}$) and settings of 40 kV and 20 mA.

UV/Vis spectra were recorded on a HACH DR/4000 U spectrophotometer within the 190 - 1100 nm range.

3. Results and discussion

3.1 Thermal analysis

Simultaneous TG-DTA and DSC curves of the compounds exhibit mass losses in steps and thermal events corresponding to these losses or due to physical phenomenon. The TG-DTA curves also show that the anhydrous compounds are formed up to 650 °C. The presence of iron as doping in the gel sample caused the lowering of the degradation temperature. The temperature ranges (θ), mass losses (%) and peak temperatures observed for each compound are shown in Table1.

Table 1. Temperature ranges (θ), mass losses (%) and peak temperatures observed for each compound.

Compound		TG-DTA		DSC	
		Steps		Steps	
		First	Second	First	Second
TiO_2^*	θ °C	30- 650	-		
	Loss (%)	16.24			

	Peak (°C)		97 (endo)	259 (exo; sharp)	
TiO ₂ - 1% Fe	θ °C	38-185	185-457		
	Loss (%)	13.00			
	Peak (°C)	105 (endo)	232 (exo; small)	108 (endo)	223 (exo; sharp)
TiO ₂ - 5% Fe	θ °C	30-200	200-451		
	Loss (%)	14.73			
	Peak (°C)	100 (endo)	195-370 (exo; broad)	99 (endo)	201 (exo; sharp)
TiO ₂ - 10% Fe	θ °C	30-207	207-523		
	Loss (%)	12.50			
	Peak (°C)	99 (endo)	207-352 (exo; broad)	101 (endo)	224 (exo; sharp)

* This compound was obtained in Mettler equipment.

3.2 Undoped TiO₂

The TG and DSC curves are shown in Fig. 1. The TG curve shows loss of mass of 16.24 % in the range of 30°C and 650°C. This mass loss is attributed to the release of the adsorbed water in the membrane surfaces, interstitial water, adsorbed ethanol and the thermal decomposition of the organic residues. The endothermic peak observed at 97°C in the DSC curve is due to the water loss and the exothermic peak at 259°C is attributed to the thermal decomposition of the organic matter and sintering between the nanoparticles in the xerogels and in agreement with the literature [32] and in disagreement with the reference [33]. As can be seen

in the X-ray spectra shown in Fig. 2, there are no differences in the patterns of diffraction after to heat the sample up to the temperature of 250°C and 260°C, showing that the crystalline phase is the same in both cases. In the DSC curve, the exothermic peak observed at 259°C in air atmosphere, also occurred in a N₂ atmosphere at 266 °C. The appearance of this exothermic peak in N₂ atmosphere (Fig. 3) is in disagreement with reference [34].

Figure 1. TG and DSC curves of undoped-TiO₂.

Figure 2. X-ray diffraction spectra of TiO₂ heated up to: (a) 250 °C; (b) 260 °C.

Figure 3. DSC curve of TiO₂ under N₂ atmosphere

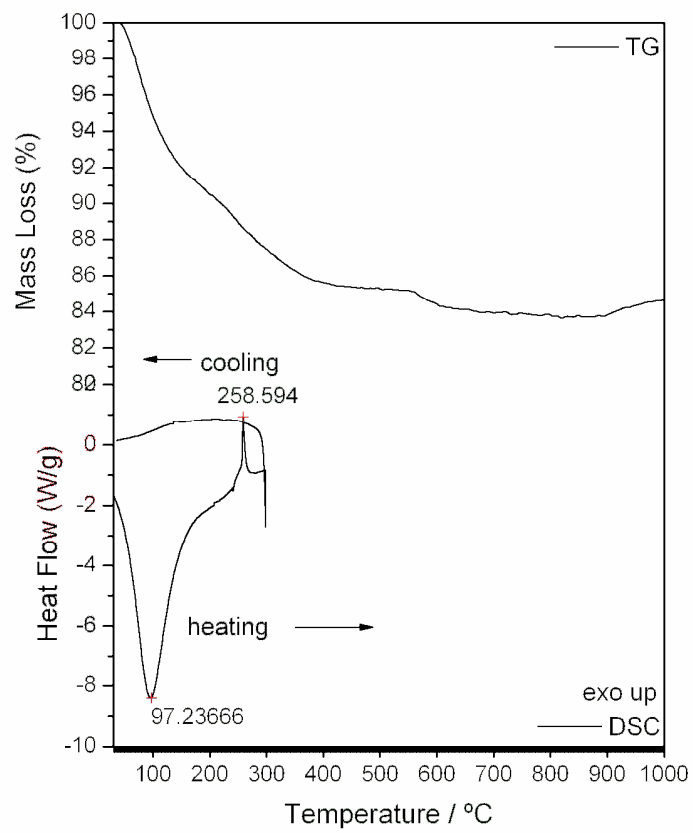


Figure 1. TG and DSC curves of undoped-TiO₂.

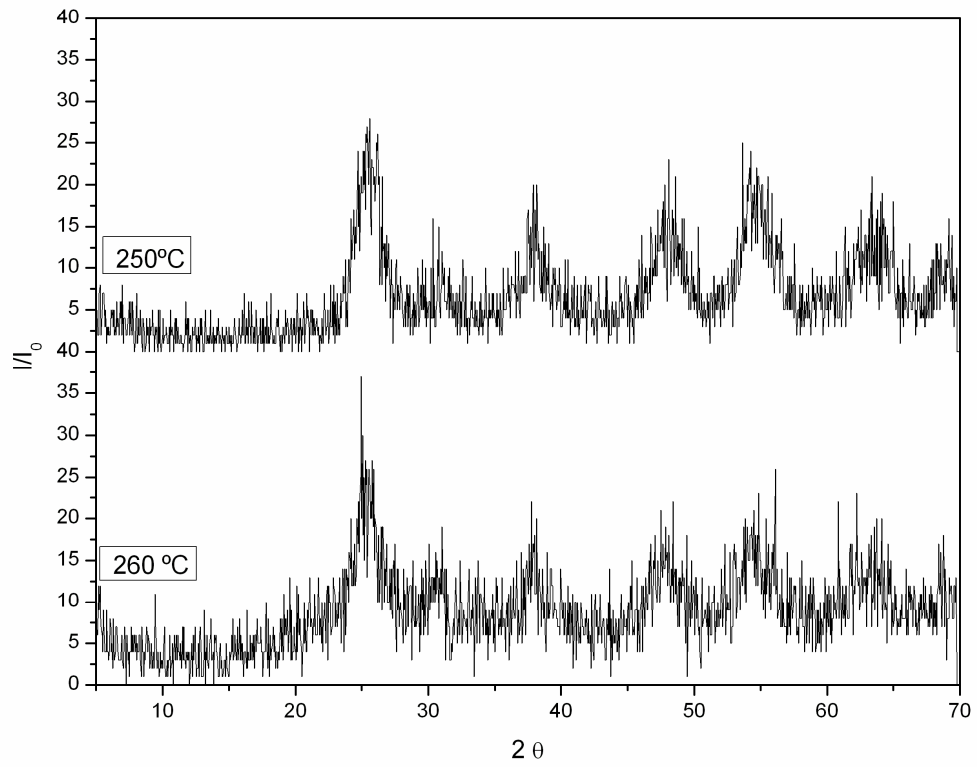


Figure 2. X-ray diffraction spectra of TiO₂ heated up to: (a) 250 °C; (b) 260 °C.

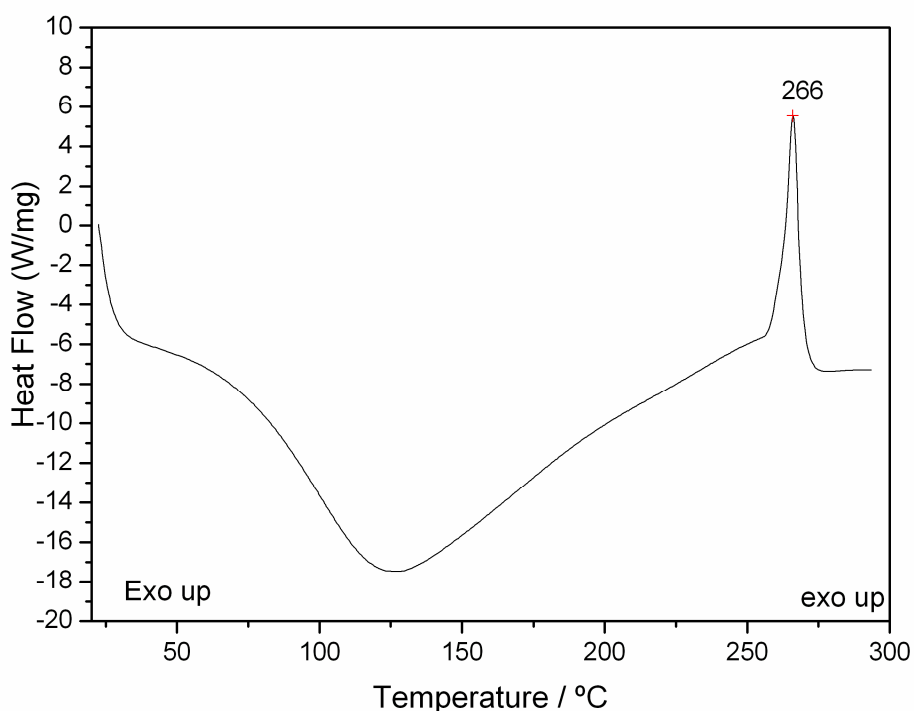


Figure 3. DSC curve of TiO_2 under N_2 atmosphere

3.3 Fe (III)-doped TiO_2

The TG-DTA and DSC curves of the titanium dioxide doped with iron (1, 5 and 10%) are shown in Figs. 4, 5 and 6. A great similarity is observed between the TG-DTA and DSC curves of the TiO_2 doped and the profile of these curves also show a great similarity with the TG-DTA and DSC curves of the titanium dioxide without doping.

However the exothermic peak attributed to the thermal decomposition of the organic matter and sintering occurs in different temperature depending on the quantity of the iron as doping (Table 1).

Figure 4. TG-DTA and DSC curves of 1% (w/w) Fe (III)- TiO_2

Figure 5. TG-DTA and DSC curves of 5% (w/w) Fe (III)- TiO_2

Figure 6. TG-DTA and DSC curves of 10% (w/w) Fe (III)-TiO₂

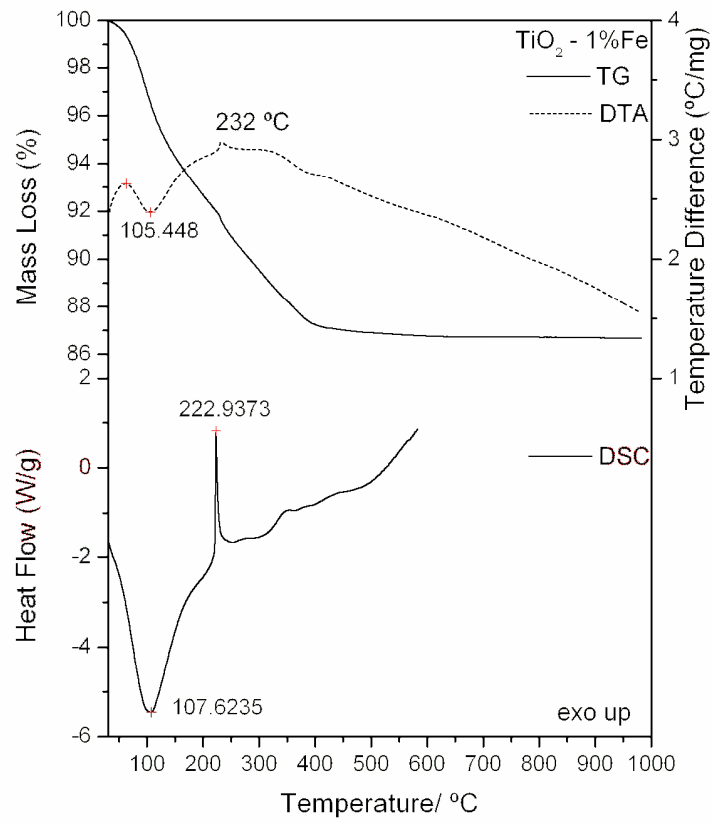


Figure 4. TG-DTA and DSC curves of 1% (w/w) Fe (III)-TiO₂

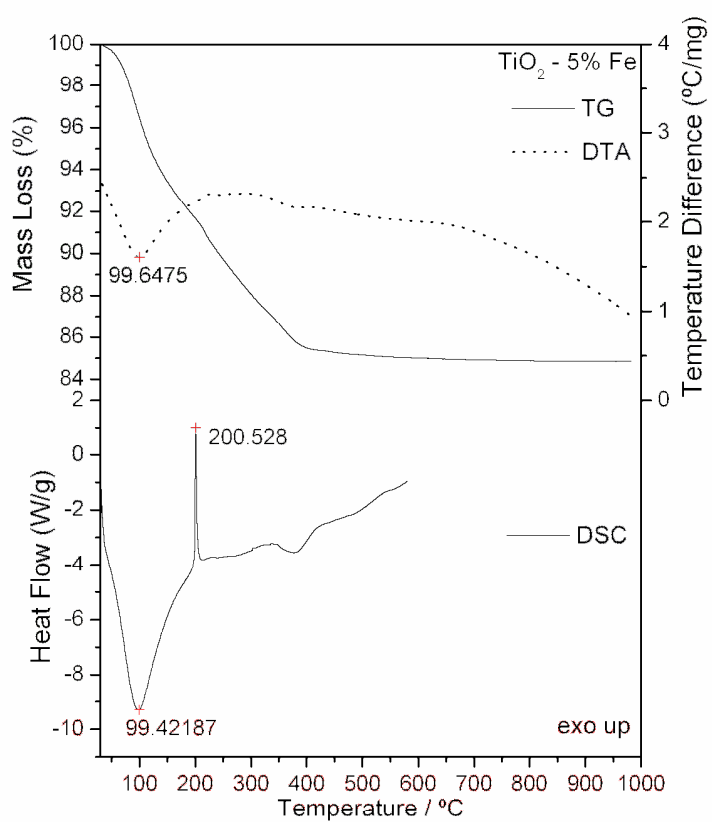


Figure 5. TG-DTA and DSC curves of 5% (w/w) Fe (III)- TiO_2

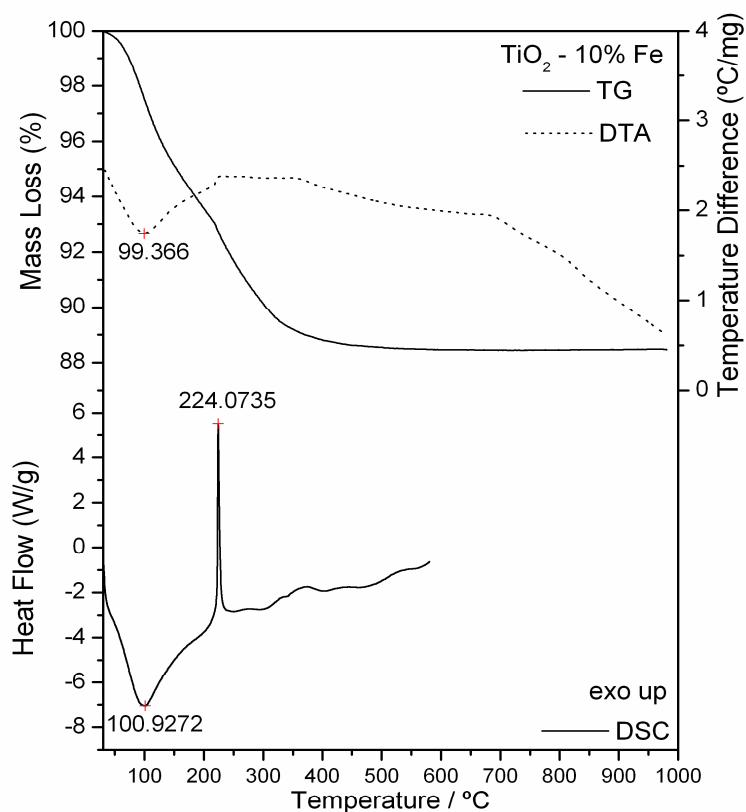


Figure 6. TG-DTA and DSC curves of 10% (w/w) Fe (III)- TiO_2

3.4 Fourier-Transformed Infrared Spectroscopy (FTIR)

IR spectra of the samples (Table 2) heated at 400 $^{\circ}\text{C}$ show a broad absorption band in the region of 1100–400 cm^{-1} corresponding to the Ti-O-Ti network [35, 36, 37]. As the iron concentration increases this band diminish its intensity and moves to longer wavenumbers. This finding is contrary to those reported elsewhere [22]. No absorption is observed in the range of 1800 cm^{-1} and 2000 cm^{-1} due to carbon bonding which is an indication of the total absence of organic compound in the samples. A broad band is observed between 1460 and 1715 cm^{-1}

attributed to O-H and Ti-OH groups. However, these two bands diminish their intensity in the iron (III) doped-TiO₂ suggesting that have occurred change in the structure of the materials.

Table 2. Infrared spectroscopic data regarding doped and undoped-TiO₂ ceramic membranes heated up to 400 °C.

Material	Wavenumber (cm ⁻¹)	
	v (O-H and Ti-OH)	v (Ti-O) and δ(Ti-O-Ti)
TiO ₂	1714-1463 ^{b; m}	1080-400 ^{b; s}
TiO ₂ - 1% Fe	1712-1460 ^{b; w}	1100-400 ^{b; m}
TiO ₂ - 5% Fe	1715-1470 ^{b; w}	1036-400 ^{b; m}
TiO ₂ - 10% Fe	1710-1480 ^{b; w}	1100-400 ^{b; m}

b – Broad; m – Medium; s – Strong; w – Weak

3.5 X-ray diffractometry

The XRD patterns of the doped- and undoped-TiO₂ powders after heating at 100 °C and 400 °C are shown in Fig. 7. The powder was amorphous when heat-treated at 100 °C. After heating at 400 °C anatase appears at $2\theta = 25.2^\circ$. At the levels of 1% and 5% of iron (III) doping the anatase peak is less intense. At the level of 10% however the peaks due to TiO₂ are bigger indicating an increase in crystallinity and particle size. Additionally, a new peak is observed at $2\theta = 25.7^\circ$ indicating a start of the phase transition.

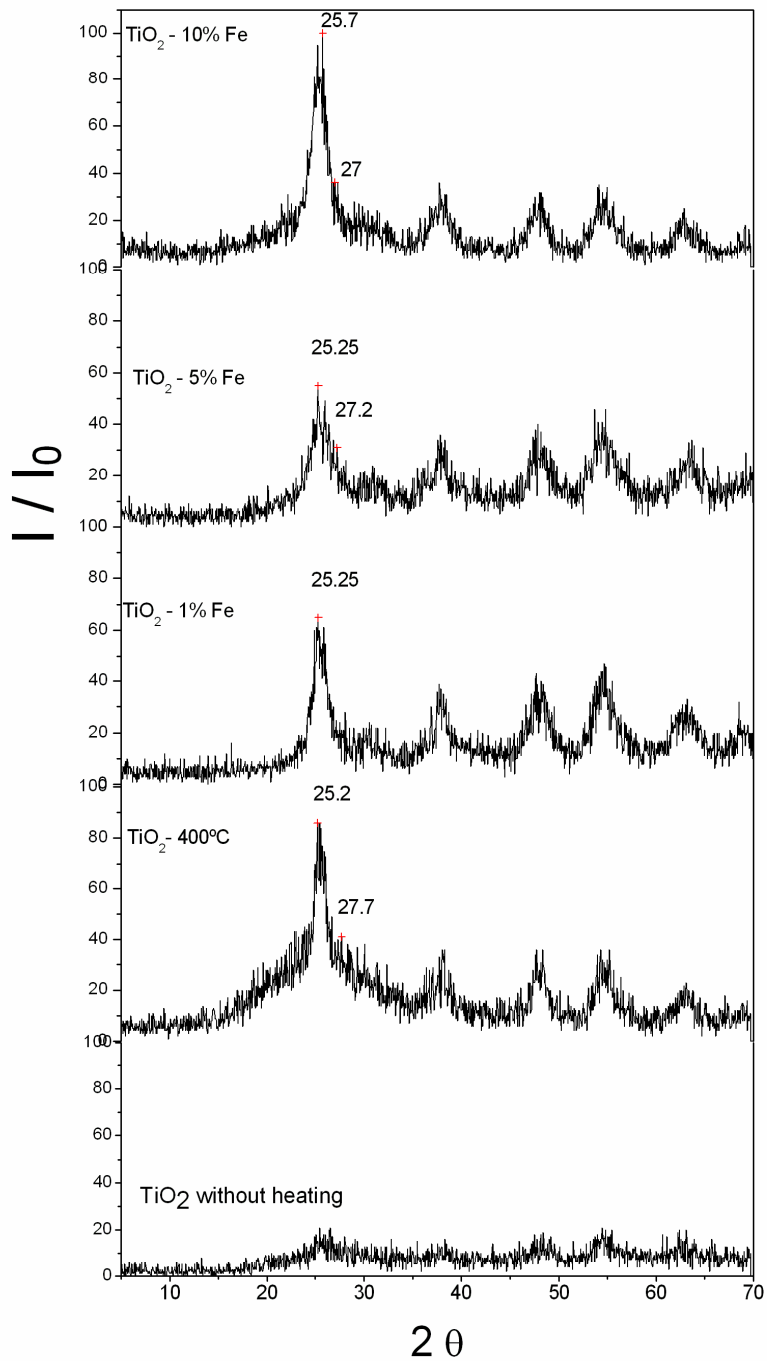


Figure 7. X-ray diffraction patterns of doped- and undoped-TiO₂.

3.6 Photoelectrocatalytic degradation of a textile dye

Thin-film electrodes made out of the iron (III) doped and undoped TiO₂ materials were used to investigate the degradation of a textile dye by photoelectrocatalyse experiment. The electrodes were made with a three layers deposition of each material on a metallic substrate of titanium with a thickness of 0.5 mm (Goodfellow Cambridge Ltd.) and heated at 400 °C for two hours. These electrodes were used as anode with a biased potential of 1.5 V (vs Ag/AgCl) and illuminated by a UV irradiation. A platinum wire was used as auxiliary electrode. The experiments were carried out for two hours in solutions of 0.05 g L⁻¹ of the dye Acid Blue 29 [5850-35-1; Aldrich] and 0.1 mol L⁻¹ NaCl as electrolyte. The variation in the dye concentration during the experiment was monitored by UV-Vis measurements.

As can be seen from Fig. 8, the dye has a characteristic peak at 602 nm which is responsible for its intense blue color. After two hours of experiment using the undoped-TiO₂ electrode this peak decreased in 36.0%. For the doped-TiO₂ electrodes the decreases were 6.37%, 27.2% and 17.2%, respectively for the 1%, 5% and 10% doping levels. Contrary to reported in the literature [38], in this case the doping metal did not improve the photocatalytic properties of TiO₂ probably due to the low temperature of 400 °C since the value most reported is 600 °C [39].

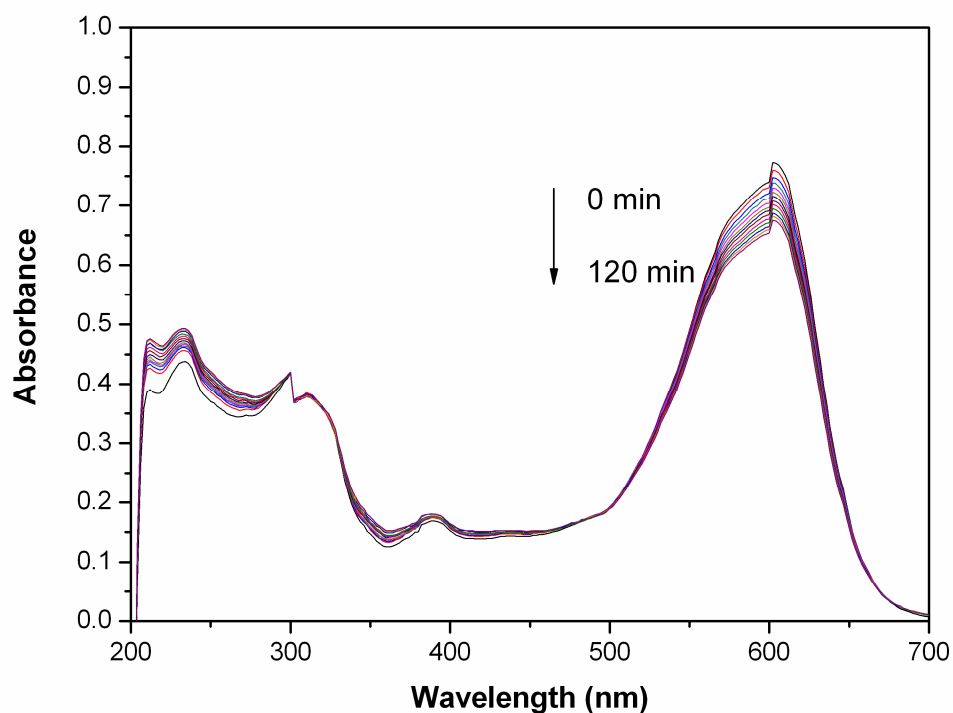


Figure 8. Variation in absorbance as a function of time during the photoelectrocatalytic degradation of the Acid Blue 29 dye using the undoped-TiO₂ thin film electrodes.

4. Conclusions

The sol-gel method has been proved to be a simple and practical way to prepare ceramic membranes of doped and undoped TiO₂. By means of thermal analysis (TG, DTA and DSC) is possible to conclude that the membranes show mass losses attributed to the release of the adsorbed water in the membrane surfaces, interstitial water, adsorbed ethanol and the thermal decomposition of the organic residues. The peaks observed in the DTA and DSC curves are due to these mass losses and sintering between the nanoparticles in the xerogels. These peaks are present in different temperature depending on the amount of iron (III) doping. The presence of the iron as metal doping in the gel caused the lowering of the mass losses and the final degradation temperature when compared with the undoped TiO₂.

X-ray diffraction allowed to observe that through heating the anatase form of TiO₂ is prevalent at the temperature studied. The doping metal has the effect of diminish the height of peaks due to TiO₂. The infrared spectra showed the presence of absorption due to Ti-O bonding. Also in the presence of the doping metal this absorption is diminished.

As a result of the photoelectrocatalytic degradation of a textile dye, plain TiO₂ remains as the best catalyst at the conditions used in this report. Among those doped catalyst, the 5% Fe (III) was able to degrade more dye than the others in the two hours of experiment.

Acknowledgements

The authors thank FAPESP, CNPQ and CAPES Foundations (Brazil) for financial support; Electroanalytical and Environmental Chemistry Group and Thermal Analysis Laboratory Ivo Giolito.

References

- [1] A. C. F. M. Costa, M. A. Vilar, H. L. Lira, R. H. G. A. Kiminami, L. Gama, *Cerâmica* 52 (2006) 255.
- [2] R. F. Silva, W. L. Vasconcelos. *Mat. Res* 5 (2002) 497.
- [3] J. J. Sene, N. R. Stradiotto, W. A. Zeltner, M. A. Anderson, W. Zhou, *Sens. Actuators, B* 87 (2002) 268.
- [4] Q. Xu, M. A. Anderson, *J. Am. Ceram. Soc.* 77 (1994) 1939.
- [5] Q. Xu, M. A. Anderson, *J. Mater. Res.* 6 (1991) 1073.
- [6] I. Truijen, M. K. Van Bael, H. Van Den Rul, J. D'haen, J. Mullens, *J. Sol-Gel Sci. Technol.* 41 (2007) 43.
- [7] Y. Li, S. H. Lim, T. White, *Int. J. Nanosci.* 3 (2004) 749.
- [8] M. M. Viana, T. D. S. Mohallem, G. L. T. Nascimento, N. D. S. Mohallem, *Braz. J. Phys.* 39 (2006) 1081.
- [9] R. A. Caruso, M. Antonietti, *Chem. Mater.* 13 (2001) 3272.
- [10] C. Airoidi, R. F. Farias, *Quim. Nova* 27 (2004) 84.

- [11] H. Yang, R. Shi, K. Zhang, Y. Hu, H. Zhang, *Int. J. Nanosci.* 5 (2006) 239.
- [12] H. Xie, T. Xi, Q. Zhang, Q. Wu, *J. Mater. Sci. Technol.* 19 (2003) 463.
- [13] R. A. Zoppo, N. H. R., Morteau, *Quim. Nova* 23 (2000) 729.
- [14] M. Crisan, A. Brăileanu, D. Crisan, M. Răileanu, N. Drăgan, D. Mardare, V. Teodorescu, A. Ianculescu, R. Birjega, M. Dumitru, *J. Therm. Anal. Cal.* 92 (2008) 7.
- [15] R. F. P. Nogueira, W. F. Jardim, *Quim. Nova* 21 (1998) 319.
- [16] A. Fujishima, T. N. Rao, D. A. Tryk, *J. Photochem. Photobiol.* 1 (2000) 1.
- [17] A. Wold, *Chem. Mater.* 5 (1993) 280.
- [18] S. Qourzal, A. Assabbane, Y. Ait-Ichou, *J. Photochem. Photobiol., A* 63 (2004) 317.
- [19] K. V. S. Rao, B. Lave´drine, P. Boule, *J. Photochem. Photobiol., A* 154 (2003) 189.
- [20] R. L. Ziolli, W. F. Jardim, *Quim. Nova* 21 (1998) 319.
- [21] J. W. J. Hamilton, J. A. Byrne, C. Mccullagh, P. S. M. Dunlop, *Int. J. Photoenergy.* 2008 (2008) 1.
- [22] M. Macek, B. Orel, T. Meden, *J. Sol-Gel Sci. Technol.* 8 (1997), 771.
- [23] T. Ohno, D. Haga, K. Fujihara, K. Kaizaki, M. Matsumura, *J. Phys. Chem. B* 101 (1997) 6415.
- [24] G. Balasubramanian, D. D. Dionysiou, M. T. Suidan, I. Baudin, J. Laîné, *J. Mater. Sci.* 38 (2003) 823.
- [25] G. Balasubramanian, D. D. Dionysiou, M. T. Suidan, I. Baudin, J. Laîné, *Appl. Catal., B* 47 (2004) 73.
- [26] V. Balek, N. Todorova, C. Trapalis, V. Stengl, E. Vecernikova, J. Subrt, Z. Malek, G. Kordas, *J. Therm. Anal. Cal.* 80 (2005) 503.
- [27] M. Asilturka, F. Sayilkana, E. Arpac, *J. Photochem. Photobiol., A* 203 (2009) 64.
- [28] Y. Wang, F. Cheng, Y. Hao, J. MA, W. Li, S. Cai, *J. Mater. Sci.* 34 (1999) 3721.
- [29] X. Li, P. Yue, C. Kutal, *New J. Chem.* 27 (2003) 1264.
- [30] X. Chen, J. Yang, J. Zhang, *J. Cent. South Univ. Technol.* 11 (2004) 161.
- [31] C. Adán, A. Bahamonde, M. Fernández-García, A. Martínez-Arias, *Appl. Catal., B* 72 (2007) 11.

- [32] E. Piera, M. I. Tjedor, M. E. Zorn, M. A. Anderson, *Appl. Catal., B* 46 (2003) 671.
- [33] K. P. Biju, M. K. Jain, *Sens. Actuators, B* 128 (2008) 407.
- [34] D. Beydoun, R. Amal, *Mater. Sci. Eng.* 94 (2002) 71.
- [35] N. S. McIntyre, K. R. Thompson, W. J. Weltner, *J. Phys. Chem.* 75 (1971) 3243.
- [36] Y. Tanaka, M. Suganuma, *J. Sol-Gel Sci. Technol.* 22 (2001) 83.
- [37] T. Ivanova, A. Harizanova, *Solid State Ionics* 138 (2001) 227.
- [38] J. W. Shi, J. T. Zheng, Y. Hu, Y. C. Zhao, *Mater. Chem. Phys.* 106 (2007) 247.
- [39] B. Tryba, *Int. J. Photoenergy.* 2008 (2008) 1.

E. C. Rodrigues, L. A. Soares, M. A. Modenes, J. J. Sene, G. Bannach, C. T. Carvalho e M. Ionashiro. Síntese e caracterização de membranas cerâmicas de dióxido de titânio dopadas com Fe(III) e sua aplicação em fotoeletrocatalise de corante têxtil.

Resumo:

Foram preparadas suspensões de TiO₂ dopadas com Fe(III) pelo método sol-gel. As propriedades dos materiais dopados foram comparadas com a de TiO₂ puro, baseadas na caracterização por análise térmica (TG-DTA e DSC), difratometria de raios X e medidas espectroscópicas (FTIR). As suspensões de TiO₂ puras e dopadas foram depositadas sobre substrato metálico, obtendo-se assim eletrodos de filme fino. O tratamento térmico destes precursors a 400 °C por um período de 2 horas resultou na formação de fase cristalina anatase. Os eletrodos foram utilizados em processo fotoeletrocatalítico para a degradação de corante têxtil em solução aquosa. Verificou-se que o eletrodo de TiO₂ puro apresentou melhor desempenho no processo de degradação do corante.

Palavras-chave: TiO₂; dopagem, caracterização, eletrodos de filme fino, corante têxtil.